Design and Surface Flashover Test of 10 kV SiC Power Module for DC Shipboard Application

Xiaoling Li
Department of Electrical Engineering
University of Arkansas
Fayetteville, USA
xl036@uark.edu

Yang Liu
School of Electrical & Computer Engineering
Georgia Institute of Technology
Atlanta, USA
yliu1024@gatech.edu

Skyler Schwartz
College of Engineering and Applied Science
University of Wisconsin-Milwaukee
Milwaukee, USA
schwa296@uwm.edu

Ning Guo
School of Electrical & Computer Engineering
Georgia Institute of Technology
Atlanta, USA
yliu1024@gatech.edu

Ebrahim Karimi
School of Electrical & Computer Engineering
Georgia Institute of Technology
Atlanta, USA
ekarimi6@gatech.edu

H. Alan Mantooth
Department of Electrical Engineering
University of Arkansas
Fayetteville, USA
mantooth@uark.edu

Lukas Graber
School of Electrical & Computer Engineering
Georgia Institute of Technology
Atlanta, USA
lukas.graber@ece.gatech.edu

Robert Cuzner
College of Engineering and Applied Science
University of Wisconsin-Milwaukee
Milwaukee, USA
cuzner@uwm.edu

2023 IEEE Energy Conversion Congress and Exposition (ECCE) | 979-8-3503-1644-5/23/$31.00 ©2023 IEEE | DOI: 10.1109/ECCE53617.2023.10362040

***Abstract*— Future all-electric ships will likely use a Medium Voltage DC (MVDC) power distribution system, which has several advantages over MVAC, such as higher power density and higher reliability. As key components for power distribution systems, 10 kV power modules need to meet the insulation requirements for various fault conditions. Grounding faults can cause extremely high electric stress between the module terminals and baseplate hence resulting in surface flashover breakdown. This paper aimed at the insulation challenges of 10 kV power module for the MVDC shipboard application. The maximum voltage stresses of four typical grounding schemes are compared at single line-to-ground faults. The surface flashover tolerance of a 10 kV SiC power module is verified under steady DC voltage and the worst-case transient fault overvoltage. The experimental results can provide a reference for the MV power module insulation design and the module baseplate grounding schemes.**

Keywords—10 kV power module, surface flashover, MVDC, shipboard power system

I. Introduction

Future all-electric ships require a reliable MVDC power distribution system to ensure energy secure power and energy delivery and to enable high energy advanced weapon systems [1]. The MVDC shipboard system requires high-power and unique insulation considerations to establish a stable, reliable, and resilient microgrid [2] [3]. Compared to the conventional terrestrial power system, the MVDC shipboard system is supported by highly integrated electric power components and utilizes the ship hull as a safety ground but, at the same time, is ungrounded or very high resistance grounded from a power reference standpoint [4][5]. This characteristic of the MVDC based distribution system is a key to its energy security requirements. The incidence of a single line-to-ground fault should not cause power interruption to any part of the system. Additionally, such a system will operate continuously with a single line-to-ground fault after fault inception until, through maintenance actions, the line-to-ground fault is located and removed. During this time, the insulation systems throughout the system are subject to elevated line-to-ground voltage stress, where "ground" refers to hull potential. Hull potential, due to safety requirements, corresponds to chassis ground of power conversion and distribution equipment comprising the MVDC system. These features give rise to two specific requirements for MV power module design [6][7]: On the one hand, power density is an important requirement for shipboard applications [8][9]. This demands compact power module packaging with minimized insulation distances and high switching frequencies capability to reduce the volume of passive components [10][11]. On the other hand, sufficient insulation is required for MV power module to withstand the worst ground fault conditions and the corresponding surface flashover transient overvoltage [12][13].

While silicon (Si)-based MV power modules are technically feasible for shipboard applications, challenges arise due to their considerable power losses, limited switching frequency, and the resulting large passive components [14][15]. In contrast, SiC MOSFETs enable compact, multi-level MV applications for lower switching losses and improved switching speed [16]. The high breakdown electric field of SiC (4H-SiC 3×10^6 V/cm, Si 0.3×10^6 V/cm) allows for higher blocking voltage[17]. These characteristics of the SiC MOSFETs enable comprehensive advantages at the converter level. With high switching frequency and low switching loss, the MV power module leads to smaller footprint, enhanced system density and high control bandwidth of MV drives [18]. Thus, MV SiC power modules enable high power density and lower switching loss for shipboard applications.

To assess the feasibility of SiC MV power modules in shipboard applications, insulation capability at ground fault overvoltage transient should be addressed [19]. The unique ungrounded onboard configuration results in transient overvoltage waveforms that can be two or three times the

operating voltage. This high surge voltage leads to surface flashover and manifests as a short circuit between the power module terminals and the baseplate [20]. This waveform also exhibits a sharp steep front and high frequency oscillation that can interfere with SiC devices. While the current MV power modules are based on IEC 60664-1 and IEC61800-5 for terrestrial industrial systems, they have not been validated for MV SiC power modules in shipboard applications.

The shipboard application poses challenges to SiC MV power module packaging design, as there exist trade-offs between sufficient insulation and packaging parasitic parameters. For MVDC shipboard application, the grounding schematic plays a crucial role in determining the worst-case overvoltage and subsequently influences the power module insulation requirements. This paper presents experimental results that verified the surface flashover tolerance for a 10 kV SiC power module. Initially, a custom-designed 10 kV SiC MOSFET power module was proposed, and the corresponding insulation requirements were analyzed based on the IEC standard in Section II. Section III analyzed four typical module-capacitors grounding schemes to identify the worst-case grounding fault. In Section IV, aiming at a 10 kV SiC power module, the surface flashover tolerance of steady and fault conditions is compared during a typical single line-to-ground fault. Finally, Section V summarized the module-capacitors grounding recommendations and requirements of insulation design from surface flashover analysis.

I. Insulation Design of 10 kV Power Module

Insulation is one of key requirements for MV power modules, particularly in terms of the interface between the power module housing surface and air. This interface, characterized by a significantly lower intrinsic dielectric strength, represents a critical boundary condition. The power module surface insulation includes functional insulation between exposed terminals and basic insulation between terminals and earthed heatsinks. These design specifics of the 10 kV SiC MOSFETs power module are listed in TABLE I [21]. The target maximum DC-link voltage is 7.2 kV with an impulse withstand voltage of 18.6 kV. The internal insulation between the chips and heat sink within an encapsulant is realized by the stacked substrates, as shown in Fig. 1.

TABLE I Specifications of the Medium Voltage Power Module.

Parameter	Value
DC-link voltage	6 kV – 7.2 kV
AC current (rms)	60 A
Switching frequency	10 kHz
Overvoltage Category	3
Pollution Degree	2
Altitude	≤ 2000m
Housing material CTI	> 600
Required Impulse Withstand Voltage	18.6 kV

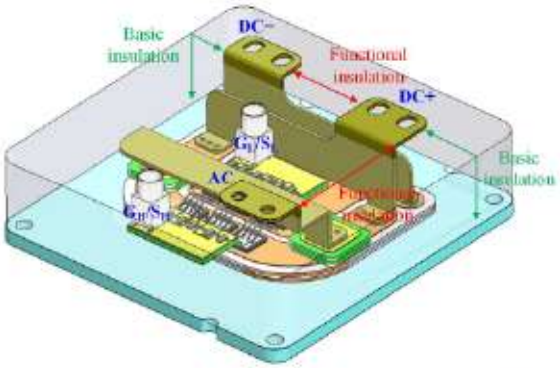

Fig. 1 Functional and basic insulation requirements of the proposed 10 kV power module.

These insulation requirements shape the parasitic inductance and parasitic capacitance within a specific module layout. The functional insulation guides the horizontal dimensions, contributing to parasitic inductance and capacitance on stacked substrates. On the other hand, basic insulation steers the vertical parasitic inductance, thereby contributing to power terminals inductance. To achieve high insulation and maintain low parasitics, a concept of arranging power module terminals based on their electrical potential is shown in Fig. 2. The terminals are categorized into three groups according to their electric potential. Group 1 includes the DC+ terminal and high-side drain, group 2 consists of the AC output terminal and high-side control terminals, and group 3 encompasses the DC− terminal and low-side control terminals. By employing the proposed electric-potential-oriented terminal arrangement, only two functional insulation distances are necessary between the three terminal groups. This arrangement successfully achieves a low parasitic inductance of 16.4 nH, and 5.3 nH with embedded decoupling capacitors. The parasitic capacitance for DC+, DC−, and AC output are 49.3 pF, 64.3 pF, and 28.1 pF, respectively.

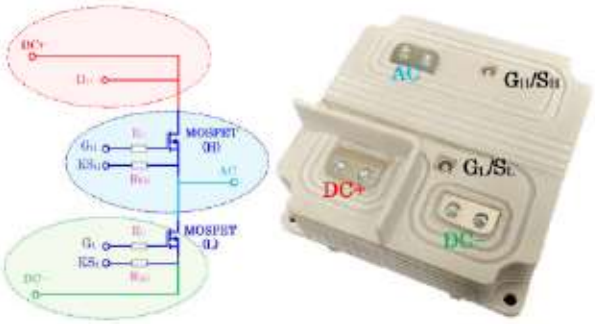

Fig. 2 Electric potential groups in a half-bridge topology.

The clearance distance and creepage distance are calculated according to IEC 60664-1 and IEC61800-5, overvoltage category III, and pollution degree II, and a material comparative tracking index (CTI) > 600. As shown in Fig. 3, the minimum terminal-terminal and terminal-baseplate clearance distance of the deisned power module is 40 mm, functional distance is 70 mm. An extra insulation wall is designed between the DC+ and DC− terminals. Creepage extenders are utilized to further increase the creepage distance.

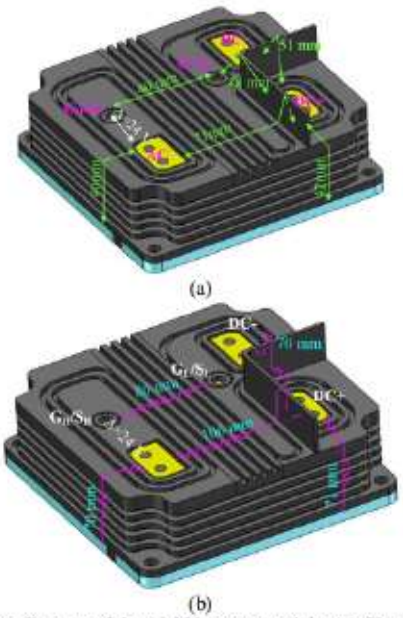

Fig. 3 Insulation distance of the 10 kV power module. (a) Clearance distance. (b) Creepage distance.

II. Electric Stress at Shipboard Grounding Fault

Since the shipboard is a mobile power system, the ship hull can be regarded as the earth ground. According to IEEE Std. 1709-2010, the power distribution system is expected to operate continuously with a single line-to-ground fault [22]. This requirement determines the insulation coordination and insulation system design requirements of all electrical components comprising the shipboard electrical distribution system [23]. The transient grounding fault can cause a peak voltage that is typically three times the normal condition. A typical grounding fault overvoltage waveform is shown in Fig. 4. The DC+ terminal withstands half of the DC link voltage of 12.5 kV before the grounding fault, and then suffers three-time $3\times V_{DC}/2$ which is 40.1 kV. For general MV power module design, a floating power module baseplate is utilized to replace the standard grounded baseplate and is explored to mitigate the insulation challenges. The floating baseplate potential is beneficial by introducing a reduced terminal-to-baseplate distance, thus reducing parasitic inductance and increasing power density at steady-state operation. However, it is prone to surface flashover breakdown at certain categories of ground faults.

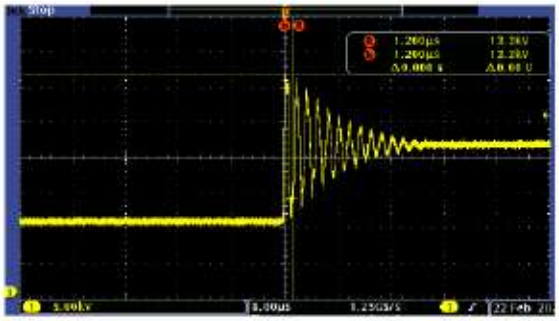
Fig. 4 Demonstration of V_{pk}(40.1kV) as greater than $3\times V_{DC}/2$ ($V_{DC}/2$ being 12.5 kV).

To determine the grounding influence on the transient electric stresses at fault conditions, four typical ground connections are compared in Fig. 5. The grounding schemes focus on the neutral point of the DC link capacitors (M) and the power module baseplate. Caused by a permanent negative rail grounding fault, transient overvoltage and steady state of the power module terminal potentials are analyzed with respect to the reference ground.

In Fig. 5(a), both M and the module baseplate are grounded to represent a traditional grounded terrestrial power system. Given a grounding fault at DC−, the potential difference between DC+ and baseplate to does not change with the fault due to the common grounding scheme. The maximum electric stress between module DC+ terminal and baseplate ΔV will keep as half of the DC link voltage ($0.5\times V_{DC}$). Similarly, for an ungrounded system in Fig. 5 (b) where M is floating yet still connected to the baseplate, although the rail-to-rail and rail-to-M voltage will be maintained as V_{DC} and $0.5\times V_{DC}$ separately, there will be a rail-to-ground voltage shifting due to the ground fault at DC−. The maximum electrical stress between module terminals to the baseplate keeps $0.5\times V_{DC}$ as the baseplate potential shift with the ungrounded middle point M. For the grounding scheme (c), both the M-point and baseplate are floating, and the two electric potentials are approximately equal due to the symmetricity of the dissipated impedance of the system. ΔV is about $0.5\times V_{DC}$ in case (c). Similarly, the worst case would be case (d) where both the neutral point M and baseplate are floating. With a DC- to virtual (e.g. cooling) ground fault, DC− will be equalized to the virtual ground-baseplate virtual point, hence DC+ will jump from $0.5\times V_{DC}$ to V_{DC} with respect to the virtual ground. With the fault short-circuiting high impedance insulations, damping will be reduced and resonance is very likely to happen, superimposing a transient peak of $0.5\times V_{DC}$ to the jump of steady state, thus the potential difference between DC+ and virtual ground (baseplate) will show the sequence of $0.5\times V_{DC}$(steady state 1)—$1.5\times V_{DC}$(transient)—V_{DC}(steady state 2). In conclusion, in case (c) and (d), the insulation between the baseplate and DC+ terminal will suffer from the peak voltage (V_{pk}), and the overvoltage level could be greater than three times the rated voltage, as shown in Fig. 4. The overall maximum electric stress under four grounding schemes is summarized in TABLE I.

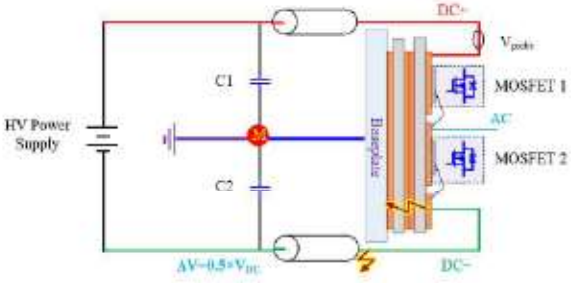

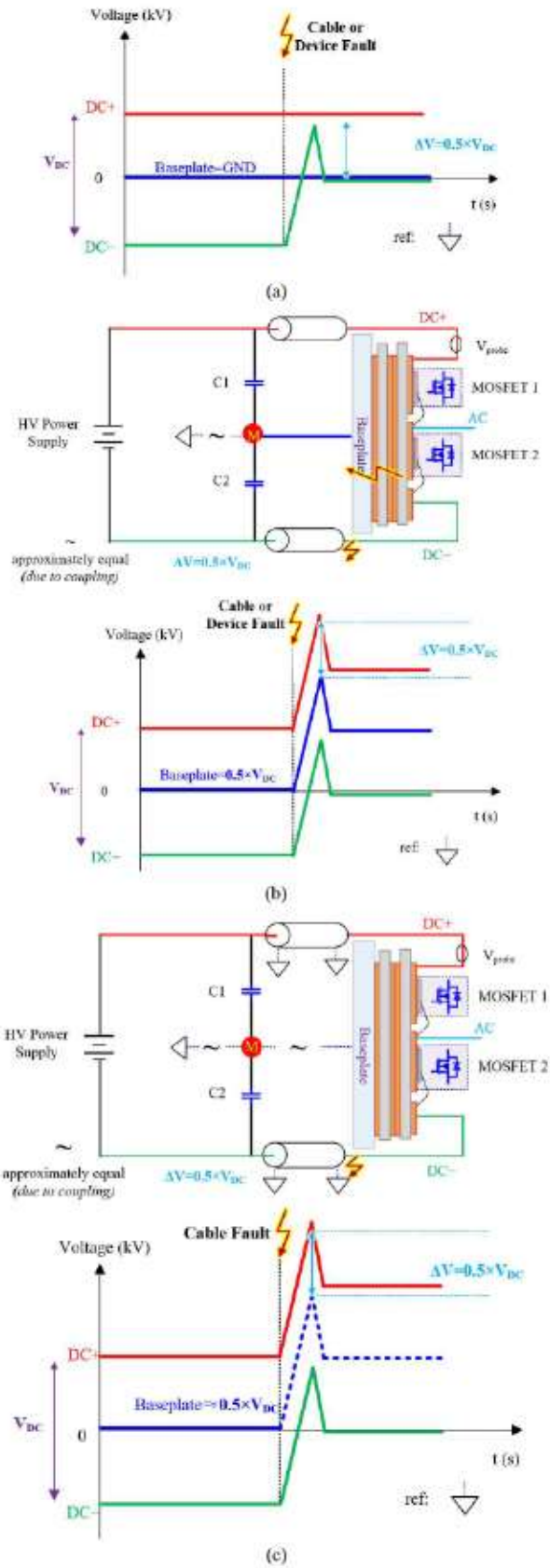

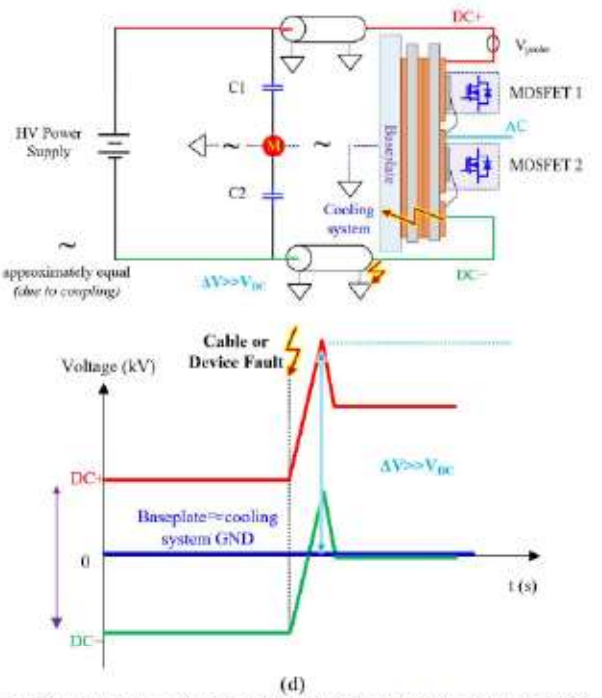

Fig. 5 Electrical stress at four grounding schemes. (a) Traditional grounded system: Neutral point M connects to GND, baseplate connects to M. (b) Ungrounded System - Neutral point connected to baseplate/cooling system ground: M float, baseplate connects to M. (c) Ungrounded System - Neutral point floating, baseplate/cooling system floating: M float, baseplate float. (d) Ungrounded System - Neutral point floating and baseplate/cooling system floating separately.

TABLE I Maximum Electric Stress under four grounding schemes.

	M connection	Baseplate connection	$\Delta V = V_{DC+} - V_{baseplate}$
(a)	GND	Connect to M = GND	$\Delta V = 0.5 \times V_{DC}$
(b)	Float	Connect to M = float	$\Delta V = 0.5 \times V_{DC}$
(c)	Float	Float approximately to M	$\Delta V = 0.5 \times V_{DC}$
(d)	Float	Float separately to M	$\Delta V \cong 1.5V_{DC}$

III. Surface Flashover Test at a 10 kV SiC Power Module

The surface flashover tolerance of the 10 kV SiC power module was tested under two different conditions: steady state DC withstanding capability and transient grounding fault tolerance. For the steady-state DC withstanding capability, the steady-state DC voltage was applied between DC+ terminals and baseplate at a ramping rate of 1%×V_{steady} (V_{steady} being estimated) per second [5] until there was a surface flashover breakdown. The steady-state DC breakdown waveform is shown in Fig. 6.

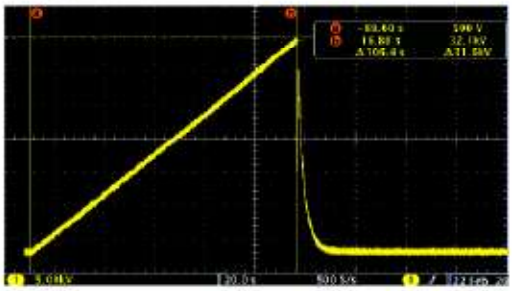

Fig. 6 Steady test waveform.

The transient surface flashover test setup is shown in Fig. 7 [6]. The surface flashover tolerance capability of a 10 kV SiC power module was tested at the worst condition, i.e., condition (d). First, S1 and S2 are connected to equally charge the DC link capacitors C1 and C2 $V_{DC}/2$[24]. The module DC+ and DC− terminals withstand V_{DC}, and the baseplate is connected to the cooling system GND. Then, S4 was close to creating a single-line-to-ground fault at the negative rail. The transient surface flashover waveform is shown in Fig. 8.

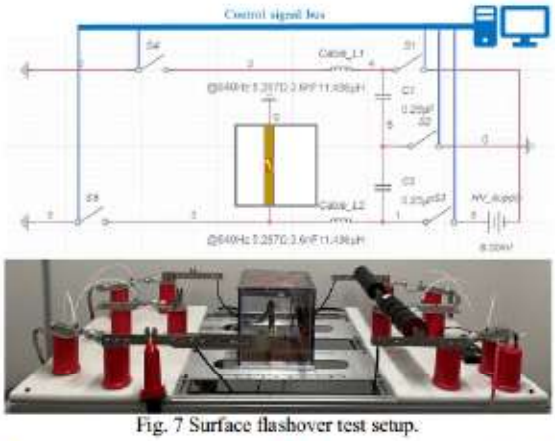

Fig. 7 Surface flashover test setup.

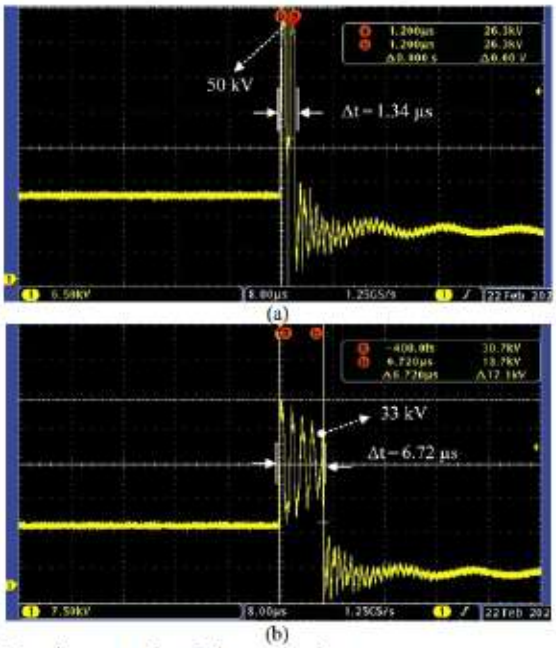

Fig. 8 Transient test surface flashover waveform.

The clearance distance and creepage distance of the tested 10 kV power module are shown in Fig. 3 (a) and (b), respectively. The clearance distance between DC+ and baseplate is 42 mm, DC− terminals and baseplate is 43 mm, AC output terminal is 40 mm. The corresponding creepage distance is 71 mm, 73mm and 70 mm. Both steady-state DC and transient grounding fault tolerance were repeated five times, the test results are shown in Fig. 9 [24].

For the DC+ terminal in Fig. 9(a), the average steady DC breakdown voltage (V_{steady}) is 33.3 kV with a maximum voltage of 33.7 kV. The average DC breakdown voltage for DC− terminals is 39.7 kV with a maximum voltage of 44.4 kV. As for the transient grounding fault tolerance test, the maximum peak voltage for both the DC+ and DC− terminals is approximately three times the DC voltage, which is coordinated with the typical waveform in Fig. 4. The DC link voltage (V_{DC}) is charged up to 25 kV, and the maximum peak voltage (V_{pk}) is higher than 40 kV. However, there was one out of five chances for no surface flashover after the ground fault, i.e., group 5 for DC+ and group 3 in DC− terminals. Nevertheless, the transient surface flashover happened at various voltage and duration conditions. As shown in Fig. 8(a), the surface flashover occurred at 1.34 μs with a peak voltage of 50 kV, while it required 6.72 μs with a peak voltage of 33 kV in Fig. 8(b). This is because the surface flashover needs to accumulate heat to mobilize space charge for the generation of surface avalanches and discharges.

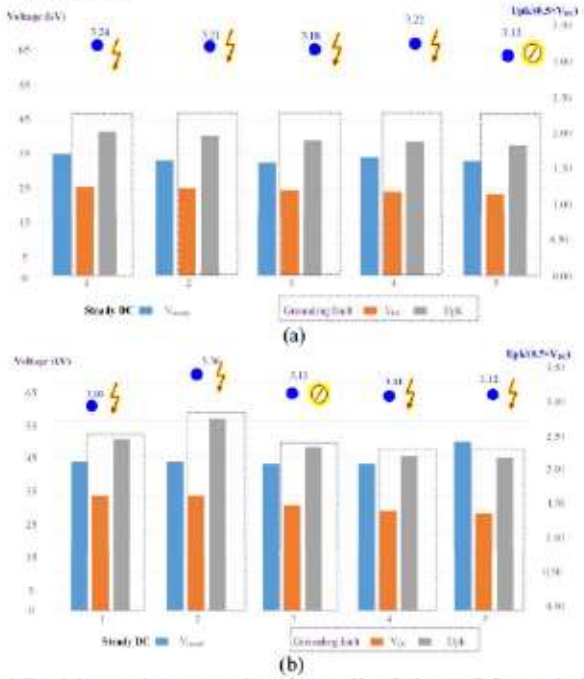

Fig. 9 Breakdown voltage at steady and grounding faults. (a) DC+ terminals. (b) DC− terminal.

In this way, the maximum safe working voltage for an MV power module should be determined by both DC and transient breakdown experimentation instead of by DC breakdown alone. Furthermore, the surface flashover time indicates that the short circuit protection should be involved within 2 μs. The photograph DC+ flashover discharge is shown in Fig. 10.

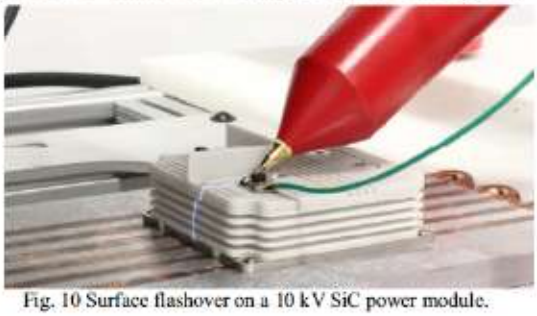

Fig. 10 Surface flashover on a 10 kV SiC power module.

IV. Conclusions

The MVDC distribution system of shipboard power systems require reliable insulation for both nominal and ground fault conditions. Aimed at a 10 kV SiC power module, the maximum terminal-baseplate electrical stresses at ground fault conditions are analyzed for different grounding schemes. The worst scenario from an insulation point of view is floating the neutral point of the DC link capacitors and grounding the baseplate to a cooling system. The surface flashover tolerance of the 10 kV SiC power module was determined under steady-state DC withstanding capability and transient grounding fault tolerance collectively. The DC+ terminal will break down at a slow ramping rate at DC voltage of 33 kV and a transient peak voltage of 40 kV with 25 kV rail-to-rail voltage. Three times of rail-to-ground voltage ($0.5\times V_{DC}$) overshot was regarded as the transient surface flashover voltage, indicating that a seemingly safe operating voltage of V_{DC} = 25kV. Therefore, surface flashover caused by ground fault should be considered in power module insulation design for shipboard MVDC applications. However, this was under perfectly clean laboratory conditions. With increasing levels of surface contamination and potentially condensate, the critical flashover voltage is expected to drop. Future work will focus on these aspects.

Acknowledgment

This work was supported by the National Science Foundation under Grant No. 1939124, GRid-connected Advanced Power Electronics Systems (GRAPES), Project GR-[1]21-04, and by the Office of Naval Research under Award No. N00014-18-1-2622. The paper was approved for public release by the Office of Naval Research under DCN#543-769-23.Any opinions, findings, and conclusions or recommendations expressed in this material are those of the author(s) and do not necessarily reflect the views of these funding agencies.

References

[1] J. Kuseian, Naval power systems technology development roadmap, Electric Ships Office, PMS 320, 2013.

[2] I. Alhurayyis, A. Elkhateb, and J. Morrow, "Isolated and nonisolated DC-to-DC converters for medium-voltage DC networks: A review," IEEE J Emerg Sel Top Power Electron, vol. 9, no. 6, pp. 7486–7500, 2021.

[3] R. M. Cuzner, V. Singh, M. Rashidi and A. Nasiri, "Converter topological and solid state protective device trade-offs for future shipboard MVDC systems," 2015 IEEE Electric Ship Technologies Symposium (ESTS), Old Town Alexandria, VA, USA, 2015, pp. 34-39.

[4] N. Zohrabi, J. Shi, and S. Abdelwahed, "An overview of design specifications and requirements for the MVDC shipboard power system," International Journal of Electrical Power and Energy Systems, vol. 104, pp. 680–693, 2019.

[5] D. Lee, D. Infante, J. Langston, S. v. Poroseva, M. Steurer, and T. Baldwin, "Grounding studies in a Medium Voltage DC shipboard power system with uncertain parameters," Grand Challenges in Modeling and Simulation Symposium, GCMS 2010 - Proceedings of the 2010 Summer Simulation Multiconference, SummerSim 2010, no. 3, pp. 113–120, 2010.

[6] J. Mohammadi, F. B. Ajaei, and G. Stevens, "Grounding the DC microgrid," IEEE Trans. Ind. Appl., vol. 55, no. 5, pp. 4490–4499, Sep./Oct. 2019.

[7] K. Choksi, Y. Wu, D. Singh and F. Luo, "Impact Assessment of common-Mode interference on communication cable in a Motor Drive System: Modified Bulk Current Injection Approach," 2023 IEEE Applied Power Electronics Conference and Exposition (APEC), Orlando, FL, USA, 2023, pp. 1769-177.

[8] R. M. Cuzner, "Power electronics packaging challenges for future warship applications," IEEE International Workshop on Integrated Power Packaging, IWIPP 2015, pp. 5–8, 2015.

[9] R. Cuzner, D. Drews, W. Kranz, A. Bendre and G. Venkataramanan, "Power-dense shipboard-compatible low-horsepower variable-frequency Drives," IEEE Transactions on Industry Applications, vol. 48, no. 6, pp. 2121-2128, Nov.-Dec. 2012.

[10] T. Damle, C. Park, J. Ding, P. Cheetham, M. Bosworth, M. Steurer, R. Cuzner, and L. Graber, "Experimental setup to evaluate creepage distance requirements for shipboard power systems," 2019 IEEE Electric Ship Technologies Symposium, ESTS 2019, pp. 317–323, 2019.

[11] A. B. Mirza, Y. Azadeh, H. Peng, Y. Li, J. Kaplun and F. Luo, "Design and validation of a MVDC isolated active voltage injection based HCB," IEEE Transactions on Industry Applications, vol. 59, no. 3, pp. 2842-2855, May-June 2023.

[12] "IEEE Standard for High-Voltage Testing Techniques," IEEE Std 4-2013 (Revision of IEEE Std 4-1995) , vol., no., pp.38, 10 May 2013.

[13] L. Xu, J. M. Guerrero, A. Lashab, B. Wei, N. Bazmohammadi, J. C. Vasquez, A. Abusorrah, "A review of DC shipboard microgrids—Part II: control architectures, stability analysis, and protection schemes," IEEE Transactions on Power Electronics, vol. 37, no. 4, pp. 4105-4120, April 2022.

[14] Y. Chen, X. Du, L. Du, X. Du, A. Hasan, X. Li, H. Chen, R. Pual, S. Chinnaiyan, Y. Zhao, H. A. Mantooth, "3.3 kV Low-Inductance Full SiC Power Module," 2023 IEEE Applied Power Electronics Conference and Exposition (APEC), Orlando, FL, USA, 2023, pp. 2634-2640.

[15] N. Jia, X. Tian, L. Xue, H. Bai, L. M. Tolbert and H. Cui, "Integrated common-mode filter for GaN power module with improved high-frequency EMI performance," IEEE Transactions on Power Electronics, vol. 38, no. 6, pp. 6897-6901, June 2023.

[16] A. N. Lemmon, R. C. Graves, R. L. Kini, M. R. Hontz, and R. Khanna, "Characterization and modeling of 10-kV Silicon Carbide modules for naval applications," IEEE J Emerg Sel Top Power Electron, vol. 5, no. 1, pp. 309–322, 2017.

[17] Z. Zhang, S. Lu, B. Wang, Y. Zhang, N. Yun, W. Sung, K. Ngo, G.Q. Lu, "Packaging of a 10-kV double-side cooled Silicon Carbide diode module with thin substrates coated by a nonlinear resistive polymer-nanoparticle composite," IEEE Transactions on Power Electronics, vol. 37, no. 12, pp. 14462-14470, Dec. 2022.

[18] I. Cvetkovic, Z. Shen, M. Jaksic, C. DiMarino, F. Chen, D. Boroyevich, and R. Burgos, "Modular scalable medium-voltage impedance measurement unit using 10 kV SiC MOSFET PEBBs," 2015 IEEE Electric Ship Technologies Symposium, ESTS 2015, pp. 326–331, 2015.

[19] Y. Liu, E. Karimi, N. A. Guo, M. Lee, and L. Graber, "Study of flashover under diverse ambient conditions mimicking MVDC shipboard power system under DC and transient voltage," 2022 IEEE Transportation Electrification Conference and Expo, ITEC 2022, pp. 491–496, 2022.

[20] L. Wang, Z. Zeng, P. Sun, S. Ai, J. Zhang, and Y. Wang, "Electric-field-dominated partial discharge in medium voltage SiC power module packaging: model, mechanism, reshaping, and assessment," IEEE Trans Power Electron, vol. 37, no. 5, pp. 5422–5432, 2022.

[21] X. Li, Y. Chen, Y. Wu, H. Chen, W. Weber, A. Nasiri, R. Cuzner, Y. Zhao, and A. Mantooth, "High voltage SiC power module optimized for low parasitics and compatible system interface," IEEE Applied Power Electronics Conference and Exposition - APEC, pp. 999–1003, 2022.

[22] K. Satpathi, A. Ukil, and J. Pou, "Short-circuit fault management in DC electric ship propulsion system: Protection requirements, review of existing technologies and future research trends," IEEE Trans. Transp. Electrific., vol. 4, no. 1, pp. 272–291, Mar. 2018.

[23] 1709-2018 Approved, IEEE Recommended Practice for 1 kV to 35 kV Medium-Voltage DC Power Systems on Ships, Nov. 2010.

[24] N. Guo, M. Lee, J. H. Choi, T. Damle and L. Graber, "Characterizing the Surface Charge Distribution and its Impact on the DC Surface Flashover Voltage of Insulators," 2021 IEEE Electric Ship Technologies Symposium (ESTS), Arlington, VA, USA, 2021, pp. 1-5.